

Mapana Journal of Sciences
2020, Vol. 19, No. 1, 71-86
ISSN 0975-3303 | <https://doi.org/10.12723/mjs.52.4>

Facile Green Synthesis of Novel Nanocarbon Materials from Agricultural Waste

Anu N Mohan* and Manoj Balachandran †

Abstract

This article highlights a novel synthesis method for the elucidation of porous graphene nanosheets (PGN) from agricultural products like wood and coconut shell charcoal. Precursors for the present study is obtained by the thermal decomposition of agricultural waste namely wood (WS) and coconut shell (CSS). The chemical modification of the carbon structures present in the samples is achieved by using a modified Hummers' method followed by extensive sonication. Analysis of chemically treated samples with various spectroscopic and microscopic techniques revealed the presence of a few layers of large-area graphene (PGN) with oxygen functionalities added to it. Agricultural waste materials are potential precursors for the large-scale synthesis of a low-cost graphene sheet and graphene quantum dots.

Keywords: Charcoal, Chemical Intercalation, Porous Graphene Nano Sheets, Mixed Structure

1. Introduction

Graphene, the wonderful nanocarbon material has innumerable applications and is the most exhilarating topic of research in the current decade [1-2]. Although graphene is a single-layered carbon, multi-layered graphene sheets have also attracted tremendous attention. In recent times, many innovative methods for the

* Department of Physics and Electronics, CHRIST (Deemed to be University), Bengaluru, India; anunmohan@gmail.com

† Department of Physics and Electronics, CHRIST (Deemed to be University), Bengaluru, India; manoj.b@christuniversity.in

synthesis of nano-structure forms of carbon such as chemical vapour deposition, micro-mechanical and microwave exfoliation of graphite, epitaxial growth, oxidative techniques and so on from a variety of precursors have been reported by many research groups [1-10]. A commonly used precursor for graphene synthesis is naturally occurring flake graphite which is purified to remove hetero-atomic contamination [7-11]. But, the complexity of flake graphite and its intrinsic defects make the precise oxidation challenging.

Oxidation destroys the sp^2 carbon network in the graphitic plane leading to the formation of sp^3 hybridised carbon, making the carbon system primarily amorphous. It also results in the formation of defect sites in the stacked graphene sheets giving it a wrinkled topography thereby enhancing the separation between individual sheets. On the other hand, successive reduction restores sp^2 content in graphene layers by the removal of sp^3 sites resulting in a higher degree of graphitisation with a few defects. Studies on the disordered carbon nanostructures affirm that the disorder in graphene can be due to the extrinsic, intrinsic defects and /or a combination of sp^2 - sp^3 carbon network [1]. This might lead to the alteration of electrochemical and mechanical properties of graphene, owing to the short-range π -interactions among the honeycomb lattice.

However, the synthesis of mixed-mode structures reported earlier from various precursors is either cumbersome or not scalable [11-15]. One could easily synthesise nanocarbon and graphene sheets in a facile way if the precursors have preformed sp^2 structures in it [2-3]. Agricultural waste products can be easily carbonised by facile techniques. This will be a novel way of converting abundantly available agricultural waste to a novel carbon material which is environmentally benign. In the present investigation, production of mixed-phase, sp^2 - sp^3 bonded, few-layer Porous Graphene Nanosheets (PGN) by taking agricultural by-product like wood and coconut shell as precursors are reported.

2. Methods

Preparation of PGN

Porous Graphene Nanostructures were prepared by carbonising wood (WS) and coconut shell by thermolytic decomposition. 2 g of WS and CSS were mixed separately with 2 g of sodium nitrate and 100 ml of sulphuric acid followed by constant stirring for 15 minutes in an ice bath. About 12 g of KMnO_4 was slowly added to the mixture by maintaining the temperature. After 30 minutes, the ice bath was removed and the solution was stirred continuously for 48 hrs with the help of a Teflon coated magnetic stirrer. This was followed by the addition of 184 ml of distilled water, 560 ml of warm water along with 40 ml of H_2O_2 and the mixture was left out for 12 hrs. The solution was washed repeatedly by centrifugation with water and acetone followed by sonication for 20 minutes and the obtained samples were designated as WS1 and CSS1. The synthesised sample intercalated by modified Hummer's method (WS1) is subjected to high-temperature pyrolysis to obtain few-layer graphene (exfoliated) (WS2); the product is further sonicated to obtain (SWS). Coconut shell charcoal was synthesised by the slow pyrolysis of coconut shell (CSS). The synthesised sample intercalated by modified Hummer's method (CSS1) and sonicated to obtain few-layer carbon structure (SCSS).

2.1 Chemical and Structural Characterisation

Spectroscopic and morphological characterisation of the samples was done using Raman spectroscopy, Scanning electron microscopy (SEM), X-ray photoelectron spectroscopy (XPS) and Electron dispersion spectroscopy (EDS). Samples were dispersed in isopropyl alcohol (IPA) and sonicated to make them a uniform suspension and spread on Si-substrate using a micropipette. Raman measurements were recorded at a wavelength of 514.5 nm using Horiba LABAM-HR spectrometer. SEM analyses of the samples were done using a JSM-6360 A (JEOL) system operated at 20 kV and a JEOL JEM-2100 model. The compositional analysis of the samples was carried out using X-ray photoelectron spectroscopy (XPS-Omicron ESCA probe). X-ray powder diffraction (XRD) patterns were obtained using a Bruker AXS D8 Advance X-ray spectrometer. The UV/Vis spectrometer (Ocean

optics JAZ series) was used for acquiring absorption spectra. Functional groups were qualitatively identified by a Fourier transform infrared spectrometer, Thermo Nicolet 370 spectrophotometer.

3. Results and Discussion

The X-ray profile (XRD) of the graphene layers from wood charcoal at different stages (WS, WS1, WS2, SWS) is presented in Fig. 1. The diffraction pattern of the synthetic graphite sample exhibits four distinctive narrow reflections in the 2θ range 10–60, 26.8° (002 plane), 42.3° (100), 44.5° (101) and 54.9° (102 plane). In contrast, the investigated samples show only two broad reflections with intensity maxima at 26.41° and 41.6° (WS), at 24.5° (WS1), at 24.77° and 43.5° (WS2) and 24.36° (SWS) respectively (Fig.1).

The peak at $\sim 26^\circ$ is referred to as π -band and is due to the presence of an aromatic ring structure. Earlier studies have attributed the presence of a peak at $\sim 42^\circ$ to hexagonal graphite lattice of multi-walled carbon nanotubes. In WS the prominent (002) peak at $\sim 25^\circ$ is owing to the graphitic carbon in the sample. In WS1 the prominent (002) peak at $\sim 25^\circ$ indicates that oxidation of WS has resulted in a heterogeneous structure with a physical mixture of graphite oxide, graphite and amorphous like carbon. The broadening of the peak can be attributed to two factors. It can be either due to the relatively short domain order of the stacked sheets or due to the small size of the layers. The spectrum also shows a low amorphous carbon content in the sample as it is evident from the low intensity of the γ band (42°).

The XRD result of the sonicated sample (SWS) shows the formation of few-layer graphene as is evident from the appearance of the peak at $\sim 14^\circ$. This is due to the increase in separation between the layers. The intensity ratio of the I_{20}/I_{26} is a measure of the quality and the degree of disorder in the carbon nanostructures in the sample. The intensity ratio of the two bands changing from 0.921 to 0.347 suggesting high order and high quality of the carbon nanosheets (CNS) formed. The grain size, L_c and L_a , along the c -axis and a -axis that are obtained by modified Scherer equations, shows systematic change with treatment. The interlayer spacing

(d_{002}) of graphite and semi-graphite normally lies within a value of 0.3-0.39 nm. The number of aromatic lamellae and the interlayer distance (d_{002}) spacing between the lamellae is calculated. The stacking height (L_c) shows a variation in the range of 1.79 nm to 1.30 nm, while the lateral size (L_a) varies from 6.80 nm to 4.03 nm. The number of aromatic lamellae is calculated and is found to be 4 layers. This indicates the clear formation of few-layer graphene oxide (GO) in the material synthesised.

It is also noticed that the interlayer distance of the sample is changed to 0.390nm from 0.334 nm with intercalation and sonication. The higher value $d_{002} = 0.371$ nm (for WS1) is due to the incorporation of carbonyl and epoxy in graphene oxide (GO) formed.

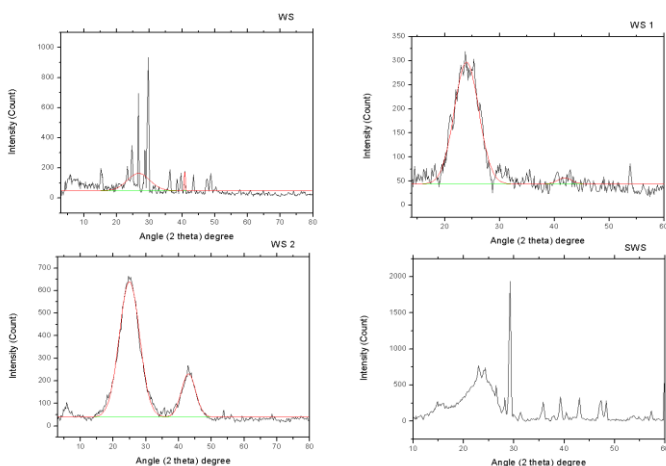


Figure 1: X-ray diffractograms of graphite from wood charcoal (WS), graphite oxide (WS1), thermally exfoliated graphene (WS2), sonicated graphene (SWS)

The Raman Spectrum of the synthesised (WS), intercalated (WS1) and exfoliated (WS2) graphene sheets are presented in Fig.2. The spectrum shows the appearance of two bands, the G-band (sp^2 - hybridised carbon-carbon bonds) and D or defect band (characteristic disordered graphite, which indicate the presence of crystalline graphitic carbon in the sample). In WS, two broad and strongly overlapping D and G bands with intensity maxima at 1338 cm^{-1} and 1583 cm^{-1} similar to graphite and broad bump (2D band)

around 2700 cm^{-1} are noticed. The intensity and position of this band are changed with intercalation and exfoliation (In WS1 - D band- 1354 cm^{-1} and G band- 1589 cm^{-1} . In WS2-D band- 1361 cm^{-1} and G band- 1587 cm^{-1}). An increase in the magnitude of D-band arises due to the incorporation of functional groups in the carbon backbone. D & G bands have slightly shifted towards higher wavenumbers as a result of oxidation. Moreover, isolated double bonds resonate at higher frequencies than the frequency of the G band of graphite. This blue shift of G band in the treated sample confirms the incorporation of oxygen functional groups.

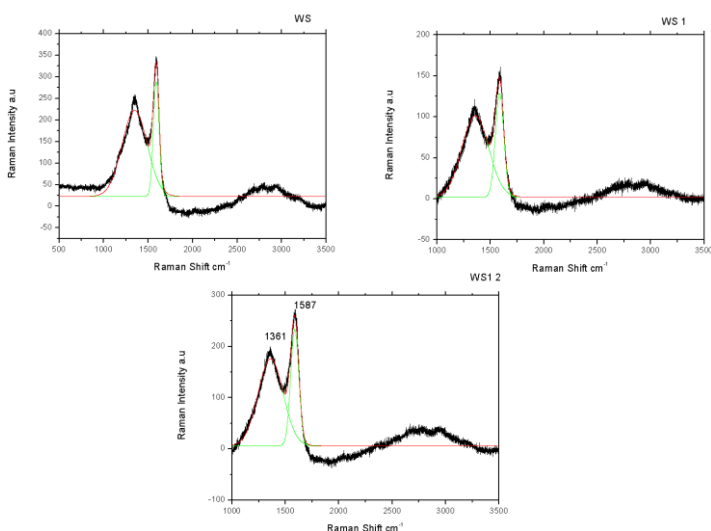


Figure 2: Raman spectrum of graphite-like material from wood charcoal (WS), graphite oxide (WS1), thermally exfoliated graphene (WS2)

The ratio between the D band and G band intensities is very low and is a good sign of the quality of the bulk samples.

FTIR spectroscopic analysis was carried out to identify the presence of a functional group in carbon nanoparticles nanostructure. Thermal decomposition of wood could produce other substances along with carbon particles. It has been reported that the atmospheric combustion of wood produces a variety of hydrocarbons along with a complex mixture of elemental carbon and other species. It consists of covalently attached oxygen-

containing functional groups (Spectra not shown), [16-17]. The carboxyl group shows its presence throughout the spectra of WS1 in the form of a broad-OH peak from 3600 to 3000 cm^{-1} , weak -OH bending at 1402 cm^{-1} , strong C-O peak at 1139 cm^{-1} and a strong C=O peak at 1714 cm^{-1} . As in the case of graphite, the carbon backbone C=C stretch can be seen at 1614 cm^{-1} . Due to the hydrogen bonding between the OH molecules, there is broadening of the -OH peak. The epoxy group's presence is shown by the C-O stretching vibration at 1041 cm^{-1} . The epoxy and -OH functional groups are attached above and below the basal planes, while the -COOH groups are bound to the edges of the basal planes.

The presence of these functional groups further confirmed by UV-Visible spectroscopy (Not shown). The two characteristic features that are exhibited by UV-Vis spectrum are a peak at ~ 300 nm (attributed to $n \rightarrow \pi^*$ transitions of C=O bonds) and a maximum at ~ 240 nm, corresponding to $\pi \rightarrow \pi^*$ transitions of C=C bonds. The XPS analysis of the product is depicted in Fig.3. The presence of the peak at ~ 286 eV is due to C-O. This C-O could be either the epoxide group (C-O-C) or the hydroxyl (C-OH) group, both of which have a similar C1s binding energy. Further, there is a considerable amount of carboxyl and carbonyl group present in GO [15-16].

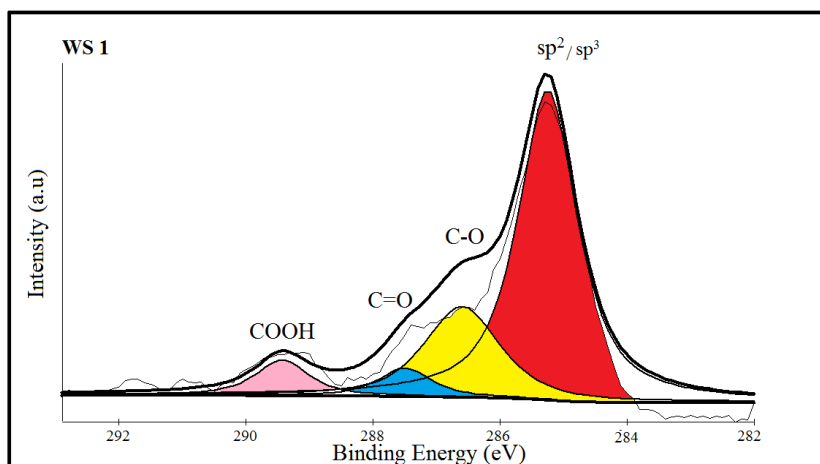


Figure 3: XPS of Graphite Oxide (WS1)

Fig.4 and Fig.5 show a FESEM image of the WS1 and WS2. The micrograph indicates the presence of micropores in the synthesised sample. With intercalation, the pore size is reduced. Micropores and nanopores are observed in the structure. The existence of nano-sized pores on the graphene flakes can be made use of in hydrogen storage and gas sensing device applications. The EDS analysis is depicted in Fig. 6. The intercalated sample shows the presence of sulphur and silicate along with carbon and oxygen. This incorporation is due to the chemical used in the intercalation.

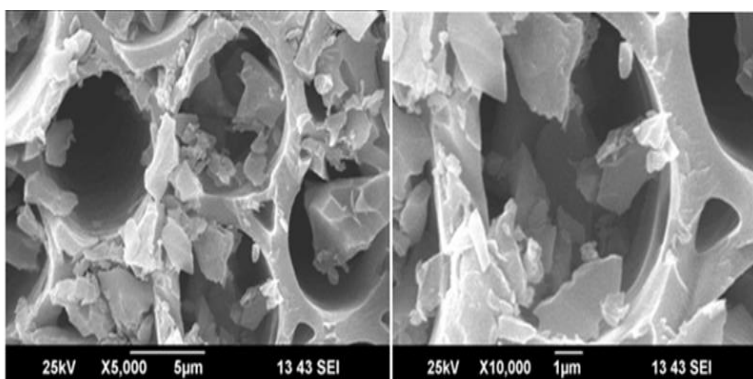


Figure 4: SEM images of graphite from wood charcoal (WS)

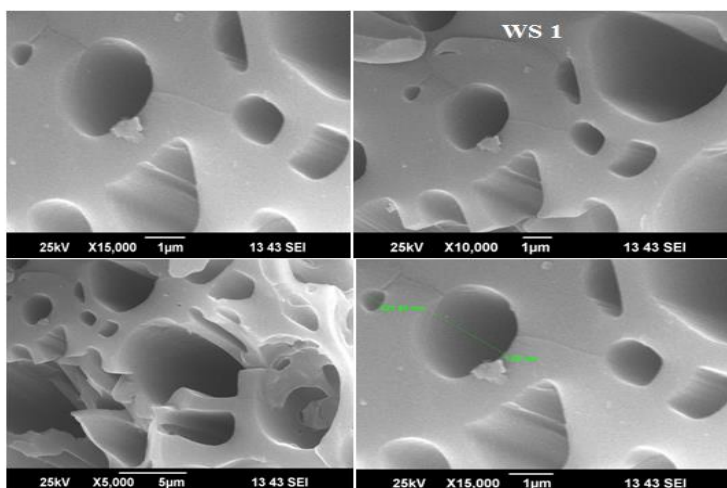


Figure 5: SEM images of graphite oxide (WS1)

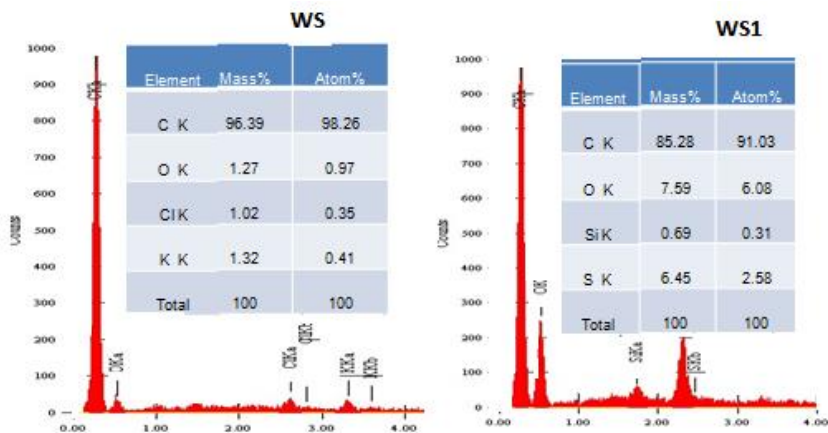


Figure 6 : EDS analysis of graphite-like carbon from wood charcoal (WS)

The EDS analysis confirmed that the content of carbon is changed to 91.03 with significant enhancement of oxygen content (6.08 wt%). The sulphur and silicates are added to the product during the treatment. The analysis confirms the incorporation of the oxygen group to carbon matrix which is in agreement with the XPS and IR analysis. The surface analysis confirms the formation of graphene-like sheets with pores from microsize to nanosize. Wood charcoal is converted to oxygenated graphene sheets in a facile synthesis way.

4. Extraction of GNC from Shell Charcoal

Graphene nanocarbon (GNC) is synthesised from carbonised charcoal and the results are presented in the section. The XRD profile shows two broad reflections with intensity maxima at 24.422° and 41.917° (CSS), at 25.109° (CSS1) and 23.95° and 42.36° (SCSS) respectively (Fig.7). The calculated structural parameters are presented in Table 3. In CSS, the prominent (002) peak at $\sim 24^\circ$ is due to the graphitic carbon in the sample. The peak at $\sim 24^\circ$ is referred to as π -band and is attributed to the presence of aromatic ring structure as described earlier. In CSS1 the prominent (002) peak at $\sim 25^\circ$ indicates that oxidation of CSS has resulted in a heterogeneous structure with a physical mixture of graphite oxide, graphite and amorphous like carbon. The spectrum also shows a low amorphous carbon content in the sample as it is evident from

the low intensity of the γ band. The broad peak at $\sim 42.35^\circ$ is attributed to the hexagonal lattice.

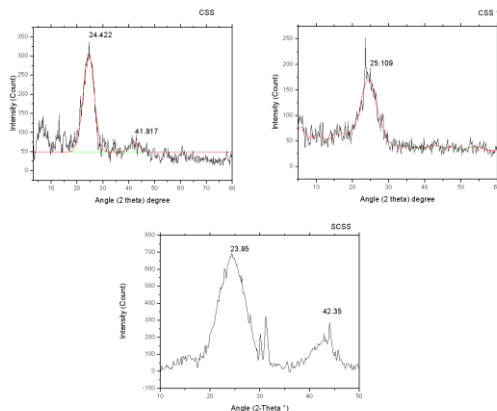


Figure 7: X-ray profile of graphite-like carbon from coconut shell charcoal (CSS), graphite oxide (CSS1), sonicated graphene (SCSS).

The intensity ratio of the I_{20}/I_{26} is a direct indication of the quality and the degree of disorder of the carbon nanostructures formed in the sample. The grain size, L_c and L_a , along c-axis and a-axis are obtained by Scherer equations and systematic change from 1.89 to 5.61 nm and 4.57 to 0.11 nm respectively with treatment. The number of aromatic lamellae is found to be ranging from 6-17 confirming multilayer stacking while the interlayer distance (d_{002}) is found to be ~ 0.36 nm.

The Raman Spectrum of the synthesised (CSS) and intercalated (CSS1) graphene sheets is presented in Fig.8. The spectrum shows the formation of two bands, the G-band around 1580 cm^{-1} (sp^2 - hybridised carbon-carbon bonds) and D or defect band around 1350 cm^{-1} (characteristic disordered graphite, which indicates the presence of crystalline graphitic carbon in the sample).

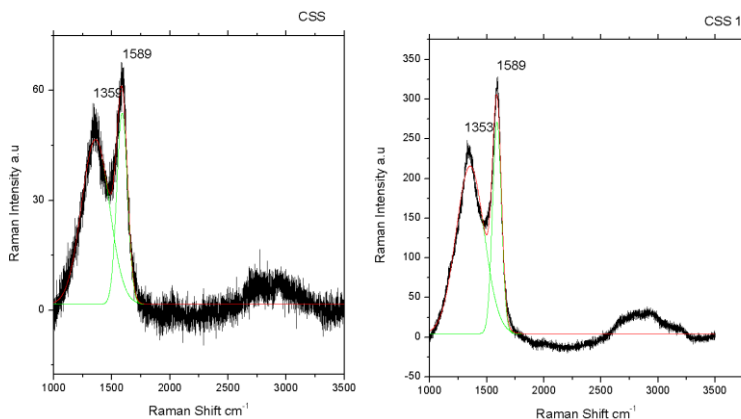


Figure 8: Raman spectrum of graphite from coconut shell charcoal (CSS), graphite oxide (CSS1)

CSS has two broad and strongly overlapping D and G bands with intensity maxima at 1359 cm^{-1} and 1589 cm^{-1} similar to graphite and a broad hump (2D band) around 2710 cm^{-1} . The intensity and position of these bands are changed with intercalation (In CSS1-D band - 1353 cm^{-1} and G band- 1589 cm^{-1}). The increase in the magnitude of D-band suggests the incorporation of functional groups in the carbon backbone (Table 4). The Blueshift of G band is observed in the treated sample thereby confirming the incorporation of the oxygen functional groups as in the case of wood charcoal. The ratio between the D band and G band intensities is a good indicator of the quality of bulk samples. The I_D/I_G ratio is found to be decreasing with the treatment indicating low disorder in the sample.

FTIR spectroscopic analysis was carried out to identify the chemical structure of carbon particles as well as the presence of any functional group in coconut shell based carbon nanoparticles (Figure not shown). It consists of covalently attached oxygen-containing groups such as hydroxyl, epoxy, carbonyl and carboxyl groups. The carboxyl group shows its presence throughout the spectra of GO in the form of a broad-OH peak from 3600 to 2000 cm^{-1} , strong C=O peak at 1710 cm^{-1} , strong C-O peak at 1139 cm^{-1} , and weak -OH bending at 1422 cm^{-1} . The carbon backbone C=C stretch can be seen at 1624 cm^{-1} as in graphite [15-20]. The broadening of the -OH peak is due to the hydrogen bonding

between the OH molecules. The C-O stretching vibration at 1039 cm^{-1} shows the presence of epoxy groups. It is generally accepted that the epoxy and -OH functional groups are attached above and below the basal planes, while the -COOH groups are bound to the edges of the basal planes.

To further confirm the presence of these functional groups, UV-Visible spectroscopy was carried out on samples dispersed in ethanol (Not shown). The $n \rightarrow \pi^*$ transitions of C=O bonds and the $\pi \rightarrow \pi^*$ transitions of C=C bonds are noticed.

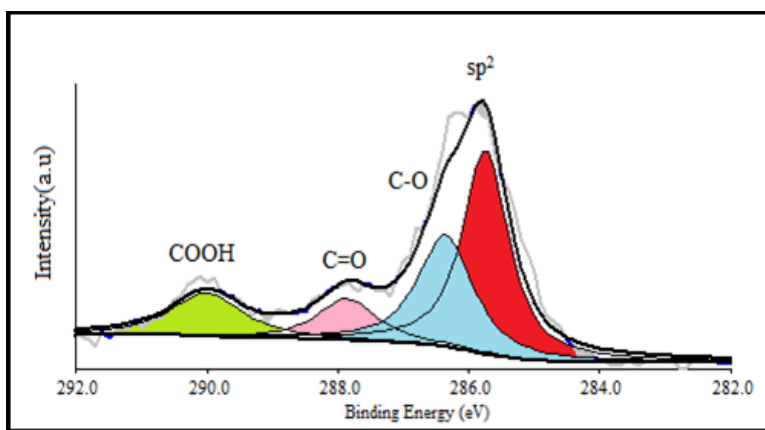


Figure 9 : XPS analysis of graphite oxide from coconut shell charcoal (CSS1)

The presence of these functional groups is confirmed by XPS analysis (Fig.9). Carboxyl, hydroxyl, carbonyl and so on are the different forms of functional groups which are introduced in GO. Further, there is a considerable amount of carboxyl and carbonyl group present in GO. The presence of a peak at ~ 286 eV is due to C-O. This C-O could be either the epoxide group (C-O-C) or the hydroxyl (C-OH) group, both of which have a similar C1s binding energy [20-24].

The surface morphology of the graphite oxide synthesised from coconut shell charcoal is depicted in Fig.10 and Fig.11. The micrograph indicates the presence of micropores and nanopores in the synthesised sample. With intercalation, the size of the pores is reduced. The existence of nano-sized pores on the graphene flakes can be made use in hydrogen storage and gas sensing device applications. The EDS analysis is presented in Fig. 12. The

intercalated sample shows the presence of sulphur and silicate along with carbon and oxygen. This incorporation is due to the chemical used in the intercalation. The content of oxygen is increased marginally due to the oxidative treatment. The obtained product is reduced graphene oxide which is an ideal precursor for the synthesis of graphene sheets, graphene quantum dots or carbon dots.

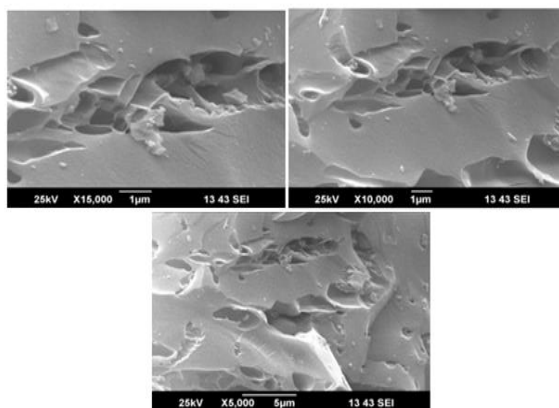
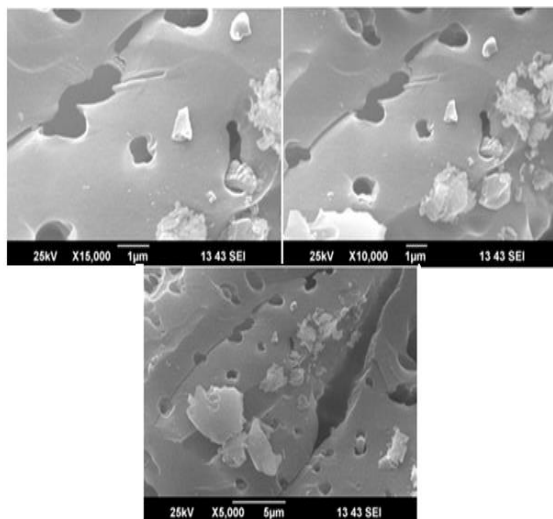


Figure 10: SEM images of graphite derived from cocnut shell charcoal



(CSS)

Figure 11: SEM images of graphitic like carbon (CSS1)

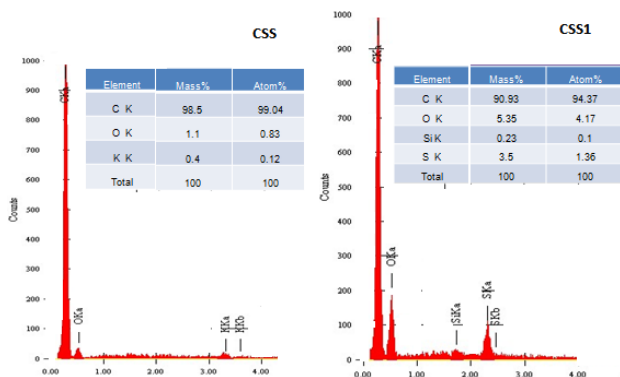


Figure 12: EDS of graphite from sonicated coconut charcoal (CSS)

5. Conclusion

Herein, the synthesis of mixed-phase, disordered few-layer graphene-like nanocarbon (GNC) from the carbonised coconut shell charcoal and soft-wood as precursors is reported. From X-ray diffraction, the presence of ordered layers of carbon network is confirmed. In the Raman analysis, variation in the intensity of peak related to graphitic (sp^2) and disordered carbon (sp^3) is observed. The presence of the 2D region indicates structural disorder in the multilayer graphene. The SEM image revealed the formation of large layers with micro and nano-sized pores. The FTIR analysis shows the C=C stretch of graphene carbon at $\sim 1624\text{ cm}^{-1}$. The presence of functional groups like OH and C=O is observed in the spectrum. The UV-Vis-NIR spectrum exhibits characterisation $\pi \rightarrow \pi^*$ transitions of C=C bonds at 240 nm and $n \rightarrow \pi^*$ transitions at C=O band at $\sim 300\text{ nm}$. Carboxyl, hydroxyl, carbonyl and so on are the different forms of functional groups which are introduced in GO. The presence of a peak at $\sim 286\text{ eV}$ is due to C-O. This C-O could be either the epoxide group (C-O-C) or the hydroxyl (C-OH) group, both of which have a similar C1s binding energy. Further, there is a considerable amount of carboxyl and carbonyl group present in GO. Although the morphology and characteristics of the graphene formed are similar, significant differences are observed in the number of functional groups. The results show softwood and

coconut shell charcoal which are agricultural wasteproduces that are converted to nanographene sheets with different properties.

References

- [1].Y. Zhu. et al., "Graphene and Graphene Oxide: Synthesis, Properties, and Applications," *Ad. Mat.*, 22:3906–3924, 2010.
- [2].B. Manoj. "Synthesis and Characterization of porous, mixed phase, wrinkled, few layer graphene like nanocarbon from charcoal" *Russian Journal of Physical Chemistry A*, 89(13): 2438-2442, 2015.
- [3].A.V.Ramya, A.N Mohan, B Manoj., "Wrinkled graphene:synthesis and characterization of few layer graphene-like nanocarbon from kerosene", *Material Science-Poland*, 34 (2):330-336, 2016.
- [4].A.K. Geim et al., "The rise of grapheme", *Mature Mat.*, 6,183-191, 2007.
- [5].Q. Liu et al., "Preparation of graphene-encapsulated magnetic microspheres for protein/peptide enrichment and MALDI-TOF MS analysis", *Chem. Comm.*, 48: 1874-1876, 2012.
- [6].A.G. Kunjomana, B Manoj, Systematic Investiagtions of graphene layers in sub-bituminous coal, *Russian Journal of Applied Chemistry*, 87(11):1726-1732, 2014.
- [7].Hummers W. et al., "Preparation of graphitic oxide", *J. Am. Chem. Soc.*, 80:1339, 1958.
- [8].B Manoj, "Chemical demineralization of high volatile Indian bituminous coal by carboxylic acid and charactetization of the products by SEM/EDS", *Journal of Environmental research and Development*. 6(3A), 2012.
- [9].A.VRamya, A.N.Mohan, B.Manoj, "Extraction and Chararcterization of wrinkled graphene nanolyers from commercial graphite", *Asian J.of Chemistry*, 28(5):1031-1034, 2016.
- [10]. S. Stankovich et al., "Synthesis of graphene-based nanosheets via chemical reduction of exfoliated graphite oxide", *Carbon*, 45:1558–1565, 2007.
- [11]. B Manoj. "Characterization of Nanocrystalline Carbon from Camphor and Diesel by X-ray diffraction technique", *Asian J. of Chemistry*, 26 (15):4553-4556, 2014.
- [12]. C.D. Elcey, B. Manoj, "Graphitization of Coal by Bio-solubilization: Structure Probe by Raman Spectroscopy", *Asian J, of Chemistry*, 28(7):1557-1560, 2016.
- [13]. B Manoj, A.M. Raj, GC Thomas, "Tailoring of low grade coal to fluorescent nanocarbon structures and their potential as a glucose sensor." *Scientific reports* 8 (1), 1-9, 2018.

- [14]. Aparna V Nair, B Manoj, "Tailoring of Energy Band Gap in Graphene-like System by Fluorination", *Mapana-Journal of Sciences* 18 (1), 55-66, 2019.
- [15]. V. L Pushparaj et al. "Flexible energy storage devices based on nanocomposite paper", *Nat. Acad. Sci. (USA)*, 104:13574-7, 2007.
- [16]. B. Manoj, C.D.Elcey, "Demineralization of coal by stepwise bioleaching: a study of sub-bituminous Indian coal by FTIR and SEM." *Journal of the University of Chemical Technology and Metallurgy* 45 (4), 385-390, 2010.
- [17]. C.D. Elcey, B. Manoj, "Demineralization of sub-bituminous coal by fungal leaching: A structural characterization by X-ray and FTIR analysis" *Research Journal of Chemistry and Environment* 17(8): 11-15, 2013.
- [18]. R.J.Nemanich et al., "First- and second-order Raman scattering from finite size crystals of graphite", *Phys Rev B*, 20: 392-401, 1979.
- [19]. Ponni Narayanan, B Manoj, "Study of Changes to the organic functional groups of a high volatile bituminous coal during organic acid treatment process by FTIR spectroscopy", *Journal of Minerals and Materials Characterization and Engineering*, 1(02):39, 2013.
- [20]. Mennella V.et al., "Raman spectra of carbon based materials excited at 1064 nm", *Carbon*. 33:115-2, 1995..
- [21]. A. Sadezky et al., "Raman microspectroscopy of soot and related carbonaceous materials: Spectral analysis and structural information", *Carbon*.43: 1731-1742, 2005.
- [22]. B Manoj, AM Raj, GT Chirayil., "Facile synthesis of preformed mixed nano-carbon structure from low rank coal." *Materials Science-Poland* 36 (1), 14-20, 2018.
- [23]. Anu N Mohan, B Manoj, Sandhya Panicker, "Facile synthesis of graphene-tin oxide nanocomposite derived from agricultural waste for enhanced antibacterial activity against *Pseudomonas aeruginosa*" *Scientific Reports*, 4170. DOI: 10.1038/s41598-019-40916-9.2019.
- [24]. B Manoj, A.M. Raj, G.T Chirayil, "Tunable direct band gap photoluminescent organic semiconducting nanoparticles from lignite" *Scientific reports* 7 (1), 1-9, 2017.